Adsorption, Lubrication, and Wear of Lubricin on Model Surfaces: Polymer Brush-Like Behavior of a Glycoprotein

Bruno Zappone,*[†] Marina Ruths,[‡] George W. Greene,* Gregory D. Jay,[§] and Jacob N. Israelachvili*

*Materials Department and Materials Research Laboratory, University of California Santa Barbara, Santa Barbara, California; [†]Centro di Eccellenza LiCryL, University of Calabria, Rende, Italy; [‡]Department of Chemistry, University of Massachusetts Lowell, Lowell, Massachusetts; and [§]Department of Emergency Medicine and Division of Engineering, Brown University, Providence, Rhode Island

ABSTRACT   Using a surface force apparatus, we have measured the normal and friction forces between layers of the human glycoprotein lubricin, the major boundary lubricant in articular joints, adsorbed from buffered saline solution on various hydrophilic and hydrophobic surfaces: i), negatively charged mica, ii), positively charged poly-lysine and aminothiol, and iii), hydrophobic alkanethiol monolayers. On all these surfaces lubricin forms dense adsorbed layers of thickness 60–100 nm. The normal force between two surfaces is always repulsive and resembles the steric entropic force measured between layers of end-grafted polymer brushes. This is the microscopic mechanism behind the antiadhesive properties showed by lubricin in clinical tests. For pressures up to ~6 atm, lubricin lubricates hydrophilic surfaces, in particular negatively charged mica (friction coefficient $\mu =$ 0.02–0.04), much better than hydrophobic surfaces ($\mu > 0.3$). At higher pressures, the friction coefficient is higher ($\mu > 0.2$) for all surfaces considered and the lubricin layers rearrange under shear. However, the glycoprotein still protects the underlying substrate from damage up to much higher pressures. These results support recent suggestions that boundary lubrication and wear protection in articular joints are due to the presence of a biological polyelectrolyte on the cartilage surfaces.

INTRODUCTION

Articular joints in the human body show excellent lubrication and wear resistance. Cartilage surfaces in synovial fluid support pressures up to ~200 atm (1), slide on each other with friction coefficients in the range 0.0005–0.04 (2) and usually do not show signs of wear over the entire life of a healthy person. However, joints do not easily heal after injury and are frequently subjected to debilitating diseases. Osteoarthritis, a degenerative disease associated with an increasing wear of the cartilage, is one of the most frequent and rapidly growing causes of permanent disability across the world, affecting more than 40 million people in the United States alone (1,3).

Joint lubrication results from a synergy of different mechanisms, both chemical and physical, acting at different length and timescales. At high rates of motion and large separations between cartilage surfaces, the highly viscous synovial fluid provides elasto-hydrodynamic lubrication (1). At cartilage-cartilage contact, water trapped in or flowing through the cartilage pores supports part of the load, producing the so-called ''weeping'' (4) or ''biphasic'' (5) lubrication. Boundary lubrication at direct cartilage-cartilage contact is provided by a glycoprotein of the synovial fluid, first purified by Radin et al. (6), and named lubricin (7). Lubricin studied in vitro lubricates cartilage sliding against cartilage (6,8), cartilage on glass (7), and latex on glass (9) as efficiently as synovial fluid. As required for an efficient boundary lubricant, lubricin binds to the cartilage surface (7), preventing cartilage-

cartilage adhesion (10). Moreover, lubricin protects the cartilage surface from excessive adsorption of proteins and cells, which is the cause of precocious joint failure in genetic diseases that affect lubricin gene expression (11).

Lubricin concentration in the synovial fluid is ~250 μg/ ml (12). Lubricin appears like a structureless, elongated, and flexible molecule with a fully extended or ''contour'' length of $l = 200 \pm 50$ nm and a diameter of a few nanometers (6,13) (shown schematically in Fig. 1). Its molecular weight $M_w = 2.3 \times 10^5$ g/mol (12) is high compared to the number of amino acids in the sequence, which is ~800 (14). This is due to the heavy glycosylation of the central portion of the molecule (Fig. 1), where short polar (-GalNAc-Gal) and negatively charged (-GalNAc-Gal-NeuAc⁻) sugar groups are O-linked to threonine residues, expressed with high frequency in 76 amino acid repeats (15). The glycosylation is almost complete and ~2/3 of the sugar groups are capped by charged sialic acid (16). The end domains of the protein are not glycosylated (Fig. 1) and contain subdomains similar to two globular proteins, somatomedin-B and homeopexin, known to play a special role in cell-cell and cell-extracellular matrix interactions (12). By analogy, we expect the end domains of the lubricin molecule to be globular, with the hydrophobic residues mainly located in the domain cores, surrounded by hydrophilic residues. At the pH = 7.2–7.6 of the synovial fluid, the molecule has a small net positive charge, the isoelectric point (IEP) being in the range 7.8–8.1 (17). Because the central domain is negatively charged, the end domains carry most of the positive charge (Fig. 1). The composition of lubricin is typical of mucin proteins, which form the mucous coating of many surfaces in the human
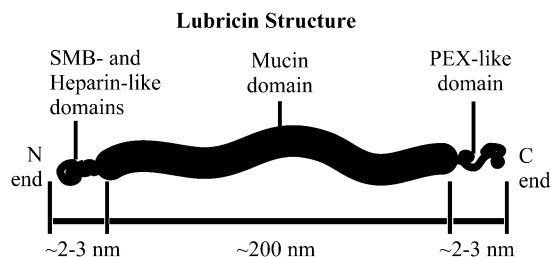
Lubricin Structure

FIGURE 1 Schematic representation of the lubricin structure. The N- and C-ends contain most of the positively charged and hydrophobic groups in the molecule and share analogies with the globular proteins somatomedin-B (*SMB*), heparin, and homeopexin (*PEX*).

body: teeth, eye-lids, respiratory and gastrointestinal tract, reproductive organs, etc. (18). Mucins bind to the epithelial surfaces and create a protective layer, often in the form of a gel. The mucin layer serves different purposes, depending on its composition and the location in the human body (18): it lubricates and prevents wear of moving surfaces such as eyelids; it reduces the adhesion of dust, bacteria, and other external agents, e.g., in the respiratory tract; it regulates permeability, e.g., in the female reproductive tract; and it resists harsh chemical conditions, e.g., in the stomach.

Recently, it was proposed (19) that protection and boundary lubrication of biological surfaces arise from a mechanism similar to that observed for brushes of end-grafted diblock polyelectrolytes. These polymers are charged in water, like proteins and polysaccharides, and are surrounded by a sheath of water molecules bound to the charged and polar groups. Polyelectrolytes show extremely low values of the friction coefficient, $\mu \sim 0.0005$, at pressures up to several atmospheres. Polyelectrolyte brushes in contact have a sharp interface, with little brush-brush interpenetration, where molecules can slide past each other interacting via the water bound to the outermost segments. When two hydration layers overlap, water moves relatively freely in the overlapping region, which effectively acts like a low viscosity lubricating fluid (20). Because it is a biological polyelectrolyte with proven boundary lubrication (6–8,13,21), lubricin is a natural candidate to test the hypothesis of a polyelectrolyte-type lubrication in biological systems (19). However, the lubricin-cartilage interaction and the lubricin's configuration on the cartilage surface are not yet understood. In fact, the composition and structure of the outermost cartilage surface itself are not completely known. This appears to consist of a soft amorphous layer of hyaluronic acid, protein, glycoprotein, and lipids (12) on top of a compact layer of type I collagen (22).

The aim of this work was to characterize the interactions between lubricin and various surfaces and to identify those that make lubricin a good boundary lubricant. Using a surface forces apparatus (SFA) we have measured the normal and friction forces between lubricin layers adsorbed on substrates with controlled chemical and physical properties: hydrophobicity, charge (both negative and positive), presence of physi-

sorbed or chemisorbed monolayers on the substrate surfaces, and roughness. Physisorbed layers of lubricin affected the frictional response and wear of all the investigated substrates. In particular, low friction coefficients in the range $\mu = 0.02$–0.04 were obtained on hydrophilic negatively charged substrates at low pressures comparable to those experienced by joint cartilage during light physical activity.

MATERIALS AND METHODS

Preparation of lubricin solutions

Human lubricin (LUB) was purified from synovial fluid according to the procedure described in Jay et al. (16). The protein was diluted at different concentrations in phosphate buffered saline ((PBS) from Sigma, St. Louis, MO; 120 mM NaCl, 10 mM phosphate salt, 2.7 mM KCl, catalog No. P3744) in aliquots of $\sim$100 μl, setting the pH within the physiological range of 7.2–7.6 (23). The solution was then stored at $-18°$C for less than four months before use. A maximum of four short freeze/thaw cycles were allowed during the sample preparation.

Substrate surfaces

Four types of reference surfaces were chosen according to their physical properties (roughness, wear-resistance) and chemical properties (charge, hydrophilicity, or hydrophobicity) in the aqueous solutions of the experiments.

Hydrophilic, negatively charged mica was chosen to model negatively charged lipids, sulphated proteoglycans, and glycoproteins found at the surface of articular cartilage (12). Muscovite mica can be cleaved by hand in the shape of transparent, uniformly thin sheets (2–5 μm thick) of area $>$1 cm². If handled and stored properly, the surface of the cleaved mica sheets is clean and atomically smooth (roughness $\sim$0.1 nm). Mica becomes negatively charged in electrolyte solutions, with a pK$_{M+}$ of 2.3–3.5 (24,25).

To mimic proteins and membranes containing basic amine groups, we have physisorbed hydrophilic positively charged poly-lysine on mica from aqueous solution. Mica surfaces were incubated overnight in a 0.05% w/w solution of polylysine ($M_w = 27,200$ g/mol, from Sigma catalog No. P4408) in deionized water. The surfaces were then rinsed in deionized water, dried in vacuum overnight (680 mm Hg at 50°C), and then dried again with N₂ gas in the SFA chamber for $\sim$1 h. To test the stability of the adsorbed poly-lysine layer in PBS, we have measured the ultraviolet (UV) adsorption of deionized water and PBS before and after dipping mica sheets coated with poly-lysine into them. Only in PBS is there measurable poly-lysine desorption, a sign that the high ionic strength of PBS weakens the electrostatic attraction between poly-lysine and the negatively charged mica surface.

A more stable monolayer of hydrophilic positively charged aminothiol was chemisorbed on gold. Using E-beam deposition, mica was first coated with 1.8 nm of Cr, and then with 7.5 nm of Au (26,27). The RMS roughness of the Au surface was 0.3 nm (3 nm maximum peak-to-peak height) over an area of $\sim$10 μm², as checked by contact-mode atomic force microscopy (AFM) in air. The surfaces were incubated for 1 h in a 4 mM solution of cysteamine (NH₂-C₂H₄-SH, from Sigma, $\geq$98%, catalog No. M6500) in ethanol, then rinsed in ethanol and blow-dried with N₂ gas. The thickness of the cysteamine layer on gold was $\sim$0.5 nm, as determined from the wavelengths transmitted at contact between thiol layers using a multilayer matrix method (27,28).

We also used hydrophobic chemisorbed (''self-assembled'') monolayers of alkanethiol on gold. This mimics the collagen below the cartilage surface, which is at least partially hydrophobic (29) and becomes exposed after severe wear of the surface. We followed the same surface preparation as above, using a 1 mM solution of hexadecanethiol (C₁₆H₃₃-SH, Fluka,

Milwaukee, WI; >95.0%) in ethanol. The thickness of the hexadecanethiol monolayer on gold was ~1.5 nm, in good agreement with previous observations (27).

Measuring forces and surface deformations with the SFA

Normal and friction forces were measured using a surface forces apparatus (model SFA3). A detailed description of the apparatus can be found in Israelachvili and McGuiggan (30). Two back-silvered sheets of muscovite mica were glued with UV-curable polyurethane glue (NOA61, by Norland, Cranbury, NJ) onto half-cylindrical glass lenses with a radius of 2 cm. The lenses were assembled in the SFA with their mica surfaces facing one another in a crossed geometry, approximating a sphere near a flat surface (see schematic *insets* in Fig. 2). Because of variations in the shape of the glue layer, the macroscopic radius of curvature of the surfaces, R, varied from experiment to experiment in the range $R = 1.8–2.2$ cm, but was not affected by the different surface treatments outlined above. To allow comparison between different experiments, the normal forces are normalized by the radius R, measured for each experiment.

The surface-surface separation distance, D, is determined with subnanometer resolution by measuring the discrete set of sharp interference fringes

selectively transmitted through the semireflecting back-silvered mica sheets (31). The distance $D = 0$ is defined by the set of wavelengths recorded at mica-mica contact in air before immersing the surfaces in solution. The interferometric setup allows measurement of the surface curvature at the contact point, and visualization of modifications, deformations, and wear (damage) of the confined film and confining surfaces occurring during the force or friction measurements. The refractive index of the medium between the surfaces can also be determined with a precision of ± 0.01.

When mica is coated with optically absorbing Cr and Au layers for supporting thiol monolayers, the standard simple optics equations (31) for calculating surface-surface separation distance D become less accurate. A more precise measurement can be obtained using a multilayer matrix method (27,28). A comparison between the two methods is shown in Fig. 8 *a*. The standard analysis gives reliable D values for $D < 50$ nm. Between 100 nm and 200 nm, the interference fringes fall in a dark region of the transmitted spectrum due to the optical absorption of the metal layers (27). In this region, the accuracy of both the standard and the multilayer method is low. In Figs. 7 and 8 *a*, we show data obtained with the standard method, keeping in mind that the distance measurements must be considered semiquantitative in the distance range between 50 and 200 nm.

To measure normal forces, F, the lower surface is attached to a horizontal double cantilever spring, which is displaced vertically toward or away from the upper surface (see *inset* in Fig. 2 *a*) with a motor-driven micrometer. As
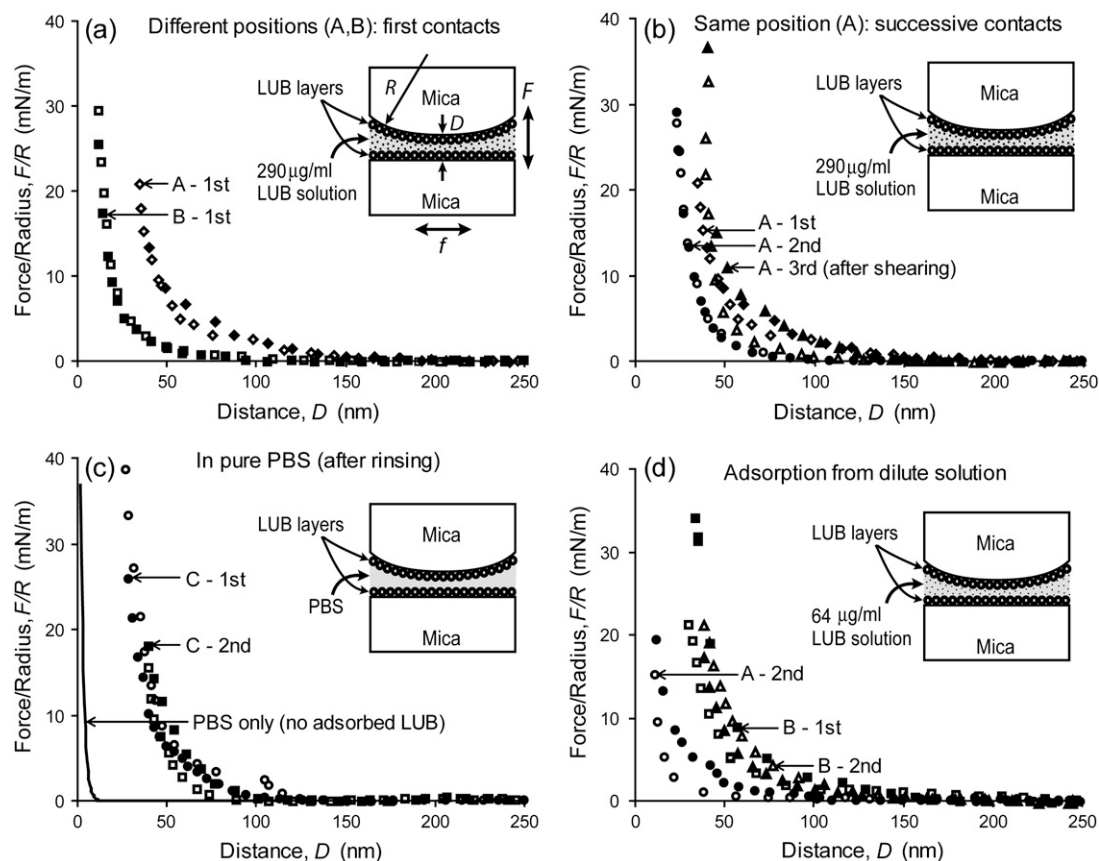

FIGURE 2 Normal forces F between negatively charged mica surfaces as a function of the mica-mica retraction D in various LUB/PBS solutions (see *insets*). The force is normalized by the radius of curvature R of the mica surfaces. Solid and open symbols indicate approaches and retractions, respectively. Force runs are chronologically labeled with a capital letter and a number: A-1st, A-2nd, B-1st, etc. The letter indicates the contact position and the number is the number of approach/retraction cycles performed at that position. (*a*) First approaches and retractions at two different contact positions, A and B. LUB concentration: 290 μg/ml (physiological). (*b*) First and subsequent approaches and retractions at the same contact position (position A of panel *a*). (*c*) Force measured after rinsing the surfaces in pure PBS solution to remove LUB from the solution. The solid line at small retractions is the force measured in pure PBS before introducing LUB in the solution. (*d*) First and subsequent approaches and retractions at different contact positions in 64 μg/ml LUB/PBS solution.

the surfaces are made to approach or retract (recede) from each other, the presence of an attractive or repulsive force causes the measured separation distance D to deviate from the one expected from a calibration of D versus motor displacement at larger distances outside the range of the interaction forces, i.e., where there is no force. This deviation is due to the vertical deflection of the spring, and is proportional to the normal force acting between the surfaces. After each approach or retraction step, one waits and observes the optical interference fringes to ascertain that all movement of the surfaces has stopped completely before D is measured, so that the equilibrium or static force is obtained. The resulting average approach and retraction rates were ~1 nm/s for $D > 150$ nm, where the interaction between the surfaces is negligible. The rate of approach and retraction was slower than 0.1 nm/s at smaller distances $D < 150$ nm, due to the surface-surface repulsion.

To measure friction forces, f, the lower surface is displaced horizontally (see Fig. 2 a) by a piezoelectric bimorph slider while the upper surface is connected to a vertical double-cantilever spring whose lateral deflection, which gives the friction force, is measured with strain gauges (32). In these experiments, the lateral sliding speed was typically 1 μm/s, as indicated in the figure legends. The normal force or load, F, is regulated with the positioning controls for moving the surfaces vertically. The force sensitivity of the apparatus used for this work was ~0.1 μN for both the normal and friction forces.

When the mica surfaces needed to be modified (as described above), the process was carried out outside the SFA, after the fringe positions corresponding to mica-mica contact ($D = 0$) were measured. After treatment, the surfaces were reassembled in the SFA and a 50–100 μl droplet of LUB solution was gently introduced between them, drawn in by capillary forces. The glycoprotein solution was then allowed to equilibrate with the surfaces for at least 3 h at room temperature. Normal and friction forces were then measured over a period of one day. After that, the surfaces were taken out of the SFA chamber and thoroughly rinsed in two or three washings of 50 ml pure PBS. The surfaces where then remounted into the SFA and the measurements resumed with the surfaces now interacting with a droplet of pure PBS solution between them. During the rinsing procedure, the surfaces were never dried or exposed to air.

An average of four contact locations were tested in each experiment. For each contact location, an average of three consecutive normal force measurements were first carried out (without shearing). The friction measurements followed the normal force measurements (unless otherwise specified). For each load, an average of three sliding cycles were used to determine the friction force. To prevent evaporation of the solution during experiments, the SFA chamber was sealed, and contained a reservoir of water that was not in direct contact with the droplet between the surfaces. If the volume of the droplet appeared to have decreased due to evaporation during experiments lasting several days, PBS or water was added to keep its volume constant. We estimate that the volume of the droplet changed by less than 30% during any experiment. All experiments were performed at 25°C.

Polymer brush interactions

The measured force-distance data was compared to the Alexander-de Gennes model (33) for the entropic repulsion between two brush layers of end-grafted uncharged polymers interacting in a good solvent. For the surface geometry in the SFA, the equation has the form (34):

$$\frac{F(D)}{R} = \frac{16\pi kTL}{35s^3}\left[7\left(\frac{2L}{D}\right)^{5/4} + 5\left(\frac{D}{2L}\right)^{7/4} - 12\right]. \quad (1)$$

The parameters L and s in Eq. 1 represent, respectively, the thickness of one brush layer and the average distance between grafting sites. The system is considered monodisperse and steric effects due to the finite size of the polymer segments are not included. These would act to increase the range of the repulsion ~2L for the same surface coverage, i.e., for the same value of s. Such ''excluded volume'' effects may be considered as an enhanced entropic or nonideal osmotic contribution to the force.

The experimental pressure (35) at the point of closest approach between the surfaces can be determined from:

$$P(D) = \frac{1}{2\pi R}\frac{\partial F}{\partial D} = \frac{kT}{s^3}\left[\left(\frac{2L}{D}\right)^{9/4} - \left(\frac{D}{2L}\right)^{3/4}\right], \quad (2)$$

where Eq. 2 is the force per area originally derived in de Gennes (33).

RESULTS AND ANALYSIS

Lubricin on hydrophilic negatively charged mica surfaces

Normal forces

Fig. 2 a shows the normal force F as a function of the separation distance D between two mica surfaces in LUB/PBS solution. Four experiments have been performed: three at a concentration 250–290 μg/ml, which is comparable with the physiological value of 250 μg/ml (12), and one at about one-quarter of the physiological concentration, 64 μg/ml. The force is purely repulsive and, depending on the experiment and the contact positions, the range of the repulsion is either ~100 nm or approximately double that value, ~200 nm. Typical forces are shown in Fig. 2, a and b. A better and more quantitative appreciation of the two distinct ranges observed is seen in the semilog plots of these forces in Fig. 3 a. Thus there appears to be two distinct conformations or states of lubricin freshly adsorbed on negatively charged mica surfaces.

The first force measurement (compression/decompression or loading/unloading cycle) at any particular contact location can show either one of the two repulsive force-distance curves (Fig. 2 a). Successive force measurements at the same location can also show either one of the force-distance curves (Fig. 2 b), although the longer repulsion tends to disappear with the time and the number of repeated contacts at the same location. The forces were reproducible during an experiment, which typically lasted a few days. The repulsion is always reversible for a compression followed by decompression, i.e., there is no hysteresis, regardless of the time the surfaces are pressed together (from 5 min to 2 h) and the magnitude of the normal force applied (up to a value of $F/R = 170$ mN/m). LUB solutions that had been frozen and stored for several months before an experiment showed only the short-range repulsion (of ~100 nm), which indicates degradation/aging of the protein solution. We only used samples less than four months old.

Fig. 2 c shows the force-distance curves obtained after rinsing the surfaces with pure PBS to remove LUB from the solution and resuming the measurements in pure PBS. The results are similar to the ones obtained before rinsing, except that only the shorter range repulsion (~100 nm) is observed. Also this force is reproducible over at least a few days, showing that it is due to a layer of LUB irreversibly adsorbed on the mica surfaces. However, the protein conformation producing the long-range repulsion (range ~200 nm) in LUB/PBS solution was removed or transformed to the
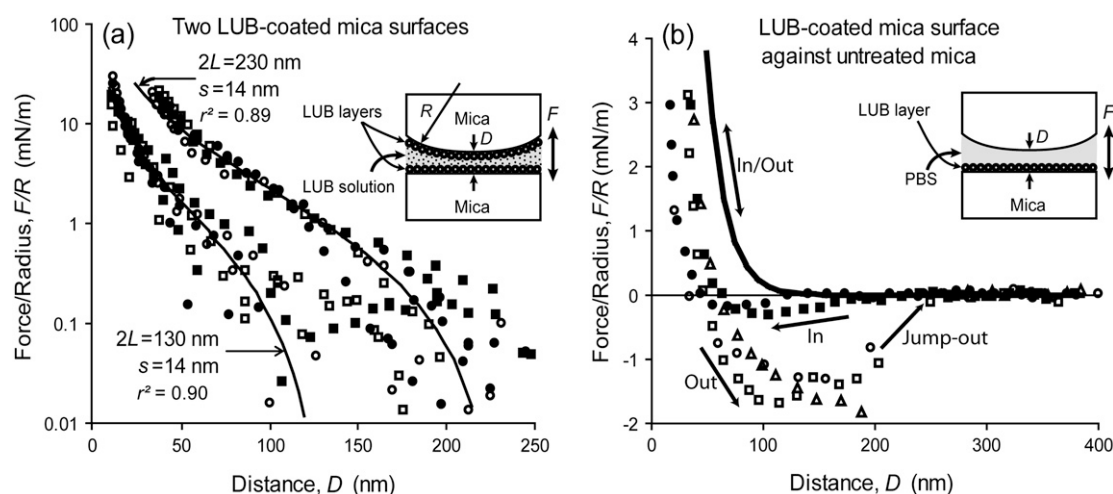
FIGURE 3 (a) Summary of the normalized normal forces F/R measured for LUB/PBS solutions between negatively charged mica surfaces. Solid ($\bullet$, $\blacksquare$) and open ($\bigcirc$, $\square$) symbols indicate approaches and separations, respectively. Circles ($\bullet$, $\bigcirc$) and squares ($\blacksquare$, $\square$) indicate LUB concentrations of 290 μg/ml (physiological; two independent experiments are shown) and 64 μg/ml (one experiment), respectively. Solid lines represent the best fits of the data to the Alexander-de Gennes model, Eq. 1, from which the values of the brush layers thickness L and the average distance between polymer binding sites s were obtained. The error in F/R is independent of D, but appears to be larger at larger separations, where the forces are weaker, due to the semilog plot used. (b) Normal forces between a LUB-coated surface and a bare (uncoated) mica surface in PBS. The results of three independent experiments are shown. The surfaces were brought into contact at different contact positions, indicated by the different symbols ($\bullet$, $\blacksquare$, $\blacktriangle$), then separated after waiting in contact from 10 min to 2h ($\bigcirc$, $\square$, $\triangle$). An arrow indicates a jump out from the ''adhesive well'' to zero force. The solid line indicates the force measured during approach and separation between two LUB-coated mica surfaces (before substituting one of the surfaces with a bare mica surface). In this case, as in Fig. 2, the force is purely repulsive both on approach and separation (minimum-maximum waiting time at contact: 5 min to 2 h), with no hysteresis and a brush layer thickness of $L \approx 65$ nm.

short-range conformation (range ~100 nm) following rinsing. For comparison, the solid line in Fig. 2 c shows the force measured between bare mica surfaces in pure PBS, before introducing LUB in the solution. This force, which is also purely repulsive, but with a much shorter range of only ~5 nm, is an electrostatic double-layer force. Its decay length corresponds to the value ~1 nm calculated based on the ionic strength of the PBS solution (36).

The adsorbed amount of LUB is expected to increase with the adsorption time and with the LUB concentration in the bulk solution. We could not detect any effect of time after the standard adsorption time of 3 h from the injection of the LUB/PBS solution between the surfaces, i.e., the adsorption appears to reach equilibrium within this time. Fig. 2 d shows the forces measured between mica surfaces 3 h after injecting a LUB/PBS solution with a concentration 64 μg/ml of about one-quarter of the physiological. No significant difference could be observed compared to the data obtained at physiological concentration (Fig. 2, a and b), including the two discrete ranges of the repulsion. Because the measured forces do not depend on the initial LUB concentration for the investigated concentrations, it may be inferred that the surface density of adsorbed LUB does not depend on the concentration either, i.e., saturation of the adsorbed amount is reached, in the form of a semidense polymer layer, and that any free (nonadsorbed) LUB in the solution has little or no effect on the measured forces. (A simple calculation shows that when the surfaces are at twice the range of the forces, ~300 nm apart, the amount of free LUB in the solution

between the surfaces is <1% of the amount adsorbed on the two surfaces, ~5 mg/m², as described below.)

The surface density of LUB adsorbed from a 250 μg/ml solution could be estimated from the refractive index n, measured as a function of the surface separation D (37). The refractive index of pure PBS is $n_{PBS} = 1.335$, as determined with an Abbé refractometer. As D is decreased to ~15 nm under an increasing load, n increases from ~n_{PBS} to 1.40–1.45. Assuming that the refractive index of LUB is $n_{LUB} \sim$ 1.5, corresponding to a refractive index increment $dn/dc = 0.18$ g/cm³ typical of proteins (38), and that the LUB density is $\rho \sim 1.0$ g/cm³, we obtain a surface mass density of ~5 mg/m², corresponding to an average distance between adsorbed molecules of $d \approx 10$ nm.

Fig. 3 a summarizes the normal forces measured between mica surfaces in LUB/PBS solution before rinsing, and shows fits of Eq. 1 to the data. Within the experimental error, the Alexander-de Gennes model (30,33) describes the magnitude, range and functional form of the experimental data well. The two distinct force-distance curves are well fitted by brush thicknesses of $L = 65$ and 115 nm, respectively, and the same grafting distance of $s \approx 14$ nm. This value compares well with the average distance between adsorbed molecules of $d \approx 10$ nm determined from the refractive index measurements. The surface mass density calculated from the value of s is 2.5 mg/m². The above analysis shows that the force is mainly of the steric-entropic type, i.e., it is due to the flexible, randomly coiled molecules that entropically resist the conformational restriction imposed by confinement (33).

Fig. 3 b shows the results of force measurements between one LUB-coated and one bare mica surface. First, LUB was adsorbed from a 250 μg/ml solution on both mica surfaces. The measured normal force followed the profile with the shorter range repulsion ($2L \approx 130$ nm), shown by the solid line in Fig. 3 b. The lower surface was then rinsed with PBS and the top one was replaced with a new bare mica surface. The surfaces were brought together in PBS and separated after waiting times of 10–120 min. On approach, the force is initially weakly attractive, then repulsive at distances D below $\sim$60 nm, i.e., roughly half of the repulsive range of $2L \approx 130$ nm between the two original (symmetrical) LUB-coated mica surfaces. On separating (retracting) the surfaces, the force becomes attractive for $D > 50$ nm, with a shallow adhesive minimum between 100 and 200 nm. Maximum adhesion of $F/R \approx -1.5$ mN/m occurs at $D \approx 200$ nm when the surfaces jump out of contact (due to the mechanical instability of the SFA setup for $dF/dD > k$, where k is the stiffness of the force-measuring spring). The adhesion is due to LUB molecules on the coated mica binding onto the opposite uncoated mica surface, giving rise to an attractive ''bridging'' force (39) that is characterized by a broad and shallow minimum before the jump out (40). The maximum bridging distance between the substrates gives a lower limit for the extended length of the molecule of $l \approx 200$ nm, which is in good agreement with previously reported values (13). The force measured on approach shows a much weaker attraction with a minimum (maximum adhesion) around -0.25 mN/m, without any detectable jump-in. This is probably due to the early stages in the formation of bridges. The attraction on approach was poorly reproducible in our experiments.

Friction forces and wear

The friction forces f as a function of the applied load F between two mica surfaces in LUB/PBS solution are presented in Fig. 4, a and b. Six independent experiments were carried out. Examples of the friction data obtained on this system are shown in Fig. 4 a, and the details of the low load regime are show in Fig. 4 b. The friction forces became measurable for separations $D = 100$–200 nm where normal (repulsive) forces also appear. However, the friction versus load curve does not depend on the range of the repulsion observed in the normal force profile (see Figs. 2 and 3 a). At loads (normal forces) up to $F \approx 0.4$ mN (contact pressure $P \approx 4$ atm; cf. Eq. 2) five experiments showed a very low friction coefficient in the range $\mu = 0.02$–0.04 (Fig. 4 b). At higher loads and pressures the friction coefficient suddenly increases by one order of magnitude $\mu = 0.2$–0.6 (Fig. 4 a). In one experiment (*solid diamonds* in Fig. 4 a), a high friction coefficient seems to be present already at low loads $F < 0.4$ mN, but not enough data points were obtained in this range to give a reliable estimate of μ. It is interesting to note that although the low friction coefficients measured at low loads were always very consistent from sample to sample (see Fig. 4 b), the high friction coefficients measured at high loads were highly scattered (Fig. 4 a).

A summary of these results and a comparison with the results obtained for other surfaces is given in Table 1 and Fig. 9.

The increased friction at higher loads ($F > 0.4$ mN, $P > 4$ atm) was always accompanied by wear of the LUB layers. When damage occurs, the film thickens by 20–40 nm (20–40% of the equilibrium film thickness) at the center of the contact area, where a smooth ''bump'' appears on the previously straight interference fringes from that area. This indicates a shear-induced clustering or aggregation of LUB molecules. The bump is never observed for loads $F < 0.4$ mN, even for the occasional measurements showing high friction right from the start of sliding. Hence, wear depends mainly on the load applied and not on the magnitude of the friction. The bump does not go away after separating the surfaces, leaving them apart for several hours, and then
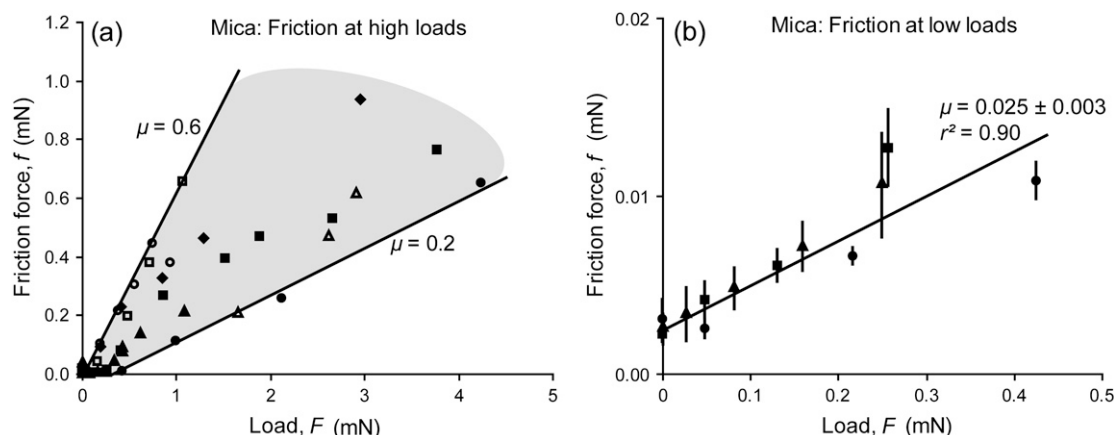

FIGURE 4 Examples of friction forces f as a function of the load (normal force) F, between two mica surfaces at the physiological LUB concentration of 290 μg/ml in PBS ($\blacksquare$, $\bullet$), at a lower concentration of 64 μg/ml ($\blacklozenge$, $\blacktriangle$), and after rinsing with PBS ($\bigcirc$, $\square$, $\triangle$). The sliding speed was $\approx$1 μm/s. (*a*) High friction coefficients, $\mu = df/dF$, at high loads. The friction data fall within the shaded area between the limits of $\mu = 0.2$ and $\mu = 0.6$. (*b*) Enlarged scale showing only the three lowest values of μ in the low load regimes of panel *a*.

TABLE 1 Mean value $\langle\mu\rangle$ and standard deviation σ of the friction coefficient $\mu = df/dF$ for each type of surface, as defined in the "Statistical summary of friction measurements" section

	Low loads	High loads
	$F < 0.4$ mN	$F > 0.4$ mN
Negatively charged, before rinsing	0.038 ± 0.018	0.28 ± 0.18
Negatively charged, after rinsing	0.22 ± 0.23	0.35 ± 0.24
Positively charged, before rinsing	0.16 ± 0.15	0.46 ± 0.13
Hydrophobic, before rinsing	0.39 ± 0.07	0.27 ± 0.08

bringing them back together again. Thus, the protein clustering/aggregation is irreversible (or the aggregates are very long-lived). The normal force measured after shearing is still repulsive, but with a larger hysteresis and a repulsion range longer than before shearing (Fig. 2 *b*), probably because of the presence of protein clusters at the center of the contact.

It is worth noting that, although LUB wears and fails to effectively lubricate mica at high loads, damage of the mica substrate itself was never observed up to loads of 8 mN (20 times higher). Apparently, LUB can continue to protect the surfaces from damage even when it has lost most of its lubricating ability.

Low friction at low loads was never clearly observed after rinsing the surfaces with PBS, nor when using LUB solutions that had been frozen and stored for more than four months. In both cases, wear appears at similar pressures (around 4 atm) as a "bump" of the same type described above.

Lubricin on physisorbed positively charged poly-lysine surfaces

Normal forces

UV-adsorption spectroscopy shows that some poly-lysine is desorbed from mica in PBS, even in the absence of LUB, due to the increased competition for the charged mica surface of the cations in the high-salt buffer solution. However, the desorption is only partial and the poly-lysine layer that is left on the surface significantly alters the properties of the mica substrate, as shown by both the normal and friction forces in LUB/PBS solution.

The normal forces measured in LUB/PBS solution (concentration 290 μg/ml) between two poly-lysine coated mica substrates (Fig. 5) show the same features observed for two mica surfaces (Fig. 2). The force is purely repulsive and there is no hysteresis on approach followed by retraction. However, in contrast to the mica surfaces, the repulsive force profiles between LUB-coated poly-lysine surfaces all show the same magnitude and range of ~150 nm, which is between the two distinct ranges measured between mica surfaces (Fig. 3 *a*). The force measured in poly-lysine solution in pure water, before introducing LUB in the solution (*dashed line* in Fig. 5 *a*), is repulsive, with a shorter range <50 nm. Hence, the repulsion observed for polylysine-coated mica in the presence of LUB is not due to the poly-lysine itself, but to the adsorption of a layer of LUB on each poly-lysine layer. The measured force in Fig. 5 *b* is well fitted by the Alexander-de Gennes model with parameters $L = 65$ nm and $s = 12$ nm if we set an offset distance $D_0 = 8$ nm in Eq. 1. This is likely to be due to the diffuse poly-lysine layer (4 nm per surface (41)) underlying the LUB layer.

Friction forces and wear

The friction between LUB layers on poly-lysine covered mica surfaces was measured as a function of the load in two different experiments. The results are shown in Fig. 6, which also shows the friction between two similar hydrophilic and positively charged aminothiol surfaces (see next paragraph). The whole range of investigated loads is shown in Fig. 6 *a* and details of the low load regime in Fig. 6 *b*. Of the two
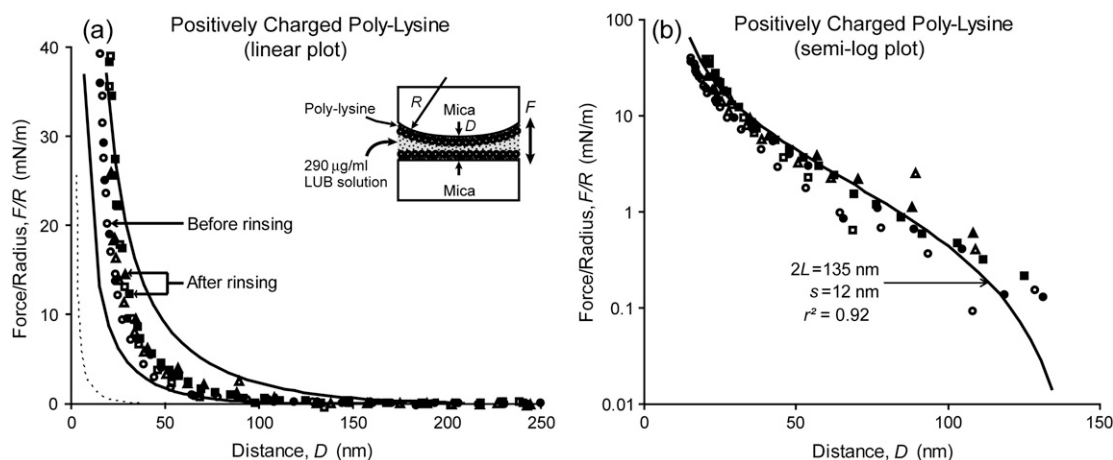

FIGURE 5 Normalized normal forces F/R as a function of the mica-mica separation D between positively charged polylysine-coated mica surfaces in LUB/PBS solution. (*a*) The solid lines in panel *a* are the two theoretical curves for LUB on bare mica from Fig. 3 *a*. The dashed line is the force between the two mica surfaces after 5 h incubation in poly-lysine/deionized water solution, before the LUB was added to the solution. (*b*) Semilog plot of the data of panel *a*. The solid line is the best fit of the Alexander-de Gennes model, Eq. 1, from which the values of the brush layers thickness L and average grafting distance s are obtained.
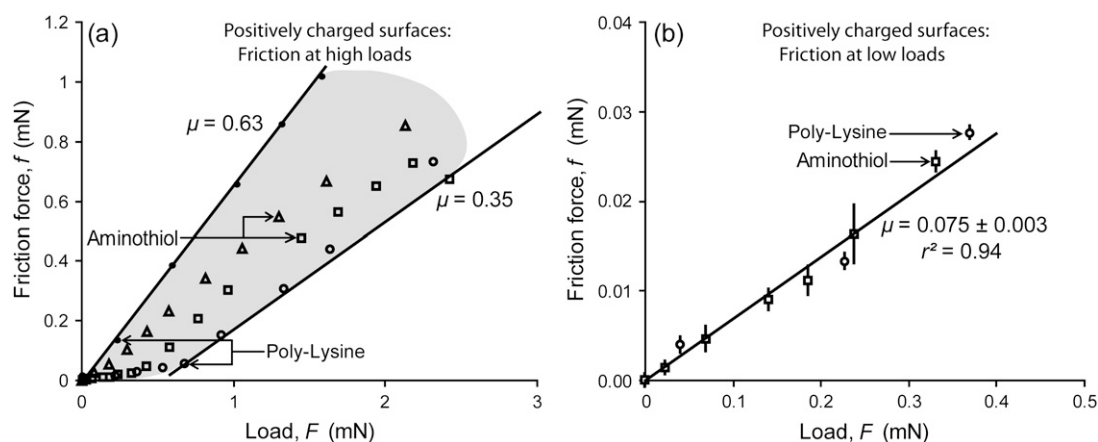
FIGURE 6   Friction forces f as a function of the load F between positively charged surfaces, poly-lysine and aminothiol, in LUB/PBS solution. The sliding speed was ≈ 1 μm/s. (*a*) High friction coefficient, $\mu = df/dF$, at high loads. The friction data fall within the shaded area between the limits of $\mu = 0.35$ and $\mu = 0.63$. (*b*) Enlarged scale showing only the two lowest values of μ in the low load regime of panel *a*.

experiments on poly-lysine surfaces, one experiment showed a low friction coefficient of $\mu \approx 0.07$ at low loads $F < 0.5$ mN ($P < 6$ atm), and a higher value of $\mu \approx 0.35$ at higher loads. For the other experiment, a high friction coefficient seems to be present already at low loads, but not enough data points were obtained in this range to give a reliable estimate of μ. The increase of the friction coefficient was always associated with irreversible aggregation of the LUB/poly-lysine layer, which nevertheless continues to protect the underlying mica from becoming worn. These results, combined with the results obtained for positively charged aminothiol surfaces, are summarized in Table 1 and Fig. 9.

Lubricin on chemisorbed positively charged hydrophilic aminothiol surfaces

Normal forces

The normal force between two aminothiol-coated gold surfaces (Fig. 7) shows features similar to those for bare mica and polylysine-coated surfaces: a repulsive force with no sign of hysteresis. The range of the repulsion varies between the two ranges observed for mica: ~ 100 nm and ~ 200 nm, without any apparent order. As described in the Materials and Methods section, the measured distances in the region $D = 50$–200 nm in Figs. 7 and 8 *a* are semiquantitative because of the reduced accuracy due to the absorption of light by the chromium-gold precoating layers.

Friction forces and wear

Two different experiments were carried out. One experiment showed a low friction coefficient, $\mu \approx 0.07$, at low loads ($F < 0.5$ mN, $P < 6$ atm) (Fig. 6 *b*) increasing to $\mu \approx 0.4$ at higher loads (Fig. 6 *a*). The other experiment showed high friction, $\mu \approx 0.4$, already at low loads (Fig. 6 *a*). The increase of μ at high loads is followed by irreversible wear, but the

damage looks different from that observed for mica and poly-lysine, appearing as a local roughening of the surface rather than as a large single smooth bump at the center of the contact. Moreover, linear wear tracks were now sometimes observed on the gold/mica surfaces along the shearing direction at the end of an experiment. The wear of the LUB layer probably leads to progressive abrasion of the gold coating, which is rougher, softer, and more prone to plastic deformations than mica (26,27). These results, combined with the results obtained for positively charged poly-lysine surfaces, are summarized in Table 1 and Fig. 9.

Hydrophobic alkanethiol surfaces

Normal forces

Freshly prepared hexadecanethiol monolayers on gold are hydrophobic to PBS and LUB/PBS solutions, which do not "wet" or spread on the surfaces (contact angle $\theta > 90°$). However, regions of the surface in contact with LUB/PBS droplets become hydrophilic after a short incubation time (<3 h), and remain so after a prolonged immersion in PBS (>24 h). The same behavior was observed on other hydrophobic surfaces such as polystyrene plates. These observations indicate that LUB adsorbs quickly and irreversibly on these surfaces, transforming them into (partially) hydrophilic surfaces.

In Fig. 8 *a*, we present the normal force measured in presence of a LUB/PBS solution at concentration 290 μg/ml (close to the physiological concentration). As for the amino-thiol surfaces, the force profiles must be considered semi-quantitative for separations in the range 50–200 nm. The normal forces were purely repulsive, with a range of ~ 100 nm and a magnitude comparable to the shorter-ranged repulsion observed for mica (brush height $2L \approx 130$ nm). No hysteresis was observed on a compression/decompression cycle. In
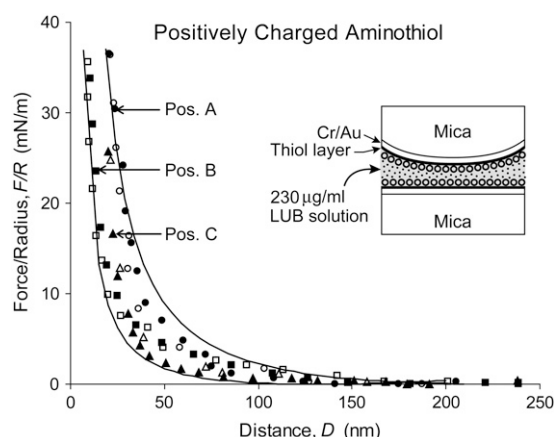
FIGURE 7 Normalized normal forces F/R between two monolayers of positively charged aminothiol on gold in LUB/PBS solution. The thiol-thiol separation D was calculated using the standard optical analysis (31), neglecting the absorbance of the metal layers. The solid lines are the two theoretical curves for LUB on bare mica from Fig. 3 a.

another experiment, the LUB concentration in PBS was set to 64 μg/ml (data not shown). The effect of bulk concentration on the normal forces was negligible, as already observed for mica.

Friction forces and wear

The friction forces between hydrophobic surfaces (Fig. 8 b) were measured in five different experiments. The results were markedly different from those observed between the charged hydrophilic mica, poly-lysine, and aminothiol surfaces. Low friction forces were never observed, even at low loads, and the friction coefficient was always between 0.3 and 0.5 as indicated in Fig. 8 b. On the other hand, the

load necessary to irreversibly wear the LUB layer was higher, ranging from 2 to 18 mN, compared to 0.4–0.5 mN for the three hydrophilic substrates. As in the case of the aminothiol surfaces, wear of the LUB appeared as a roughening of the surfaces leading to abrasion of the gold layers. A summary of these results is given Table 1 and Fig. 9.

Statistical summary of friction measurements

Table 1 and Fig. 9 show a summary of all the friction measurements presented in this work, divided into eight groups. Each group is defined as a set of independent experiments using the same type of surface (negatively charged, positively charged, or hydrophobic), in contact with the same solution (LUB/PBS before rinsing or pure PBS after rinsing) for the same load range (low loads $F < 0.4$ mN or high loads $F > 0.4$ mN). To assess the statistical relevance of the differences in the mean values of the friction coefficients of different groups, $\langle\mu\rangle$, an ANOVA test was performed on all groups. The value of the statistical significance is $p = 0.01$, indicating that there is a significant difference between at least one pair of groups. Therefore, the groups were compared pairwise, using one-sided Student t-tests to obtain the values of the significance p. This analysis showed that the following trends, shown in Table 1, are statistically relevant:

1. Before rinsing and at low loads, the mean friction coefficient for hydrophilic negatively charged surfaces, $\langle\mu\rangle = 0.038 \pm 0.018$, is one order of magnitude lower than for hydrophobic surfaces, $\langle\mu\rangle = 0.39 \pm 0.07$ ($p = 0.001$).
2. Before rinsing and at low loads, the mean friction coefficient for hydrophilic positively charged surfaces is lower than for hydrophobic surfaces ($p = 0.021$).
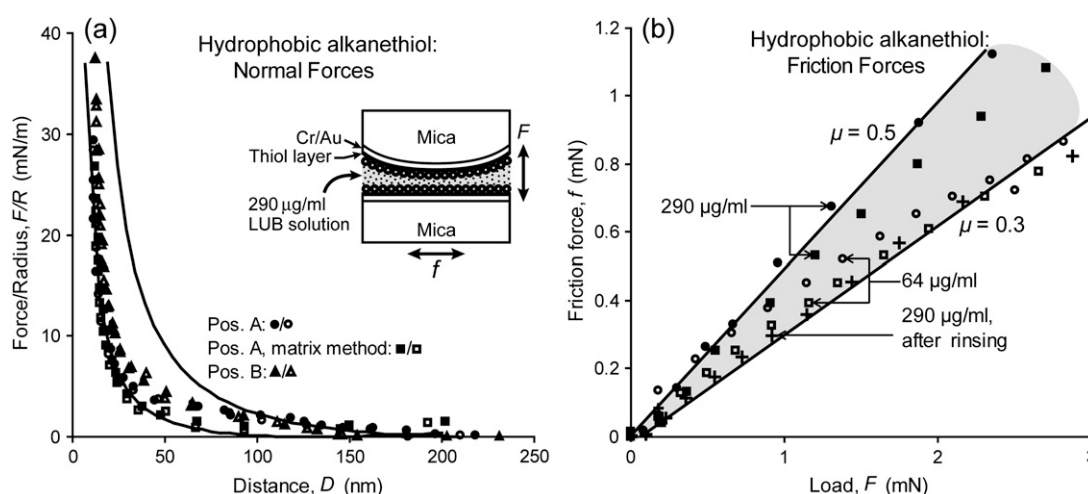

FIGURE 8 Forces between two hydrophobic monolayers of alkanethiol on gold in LUB/PBS solution. (a) Normalized normal forces F/R as a function of the thiol-thiol separation D. Square symbols ($\blacksquare$, $\square$) indicate data points obtained using the multilayer matrix method (27,28) that includes the optical absorbance of the metal layers. The solid lines are the two best-fit curves for LUB on bare mica from Fig. 3 a. (b) Friction force f as a function of the load (normal force) F. The friction data fall within the shaded area between the limits of $\mu = 0.3$ and $\mu = 0.5$. The sliding speed was ≈ 1 μm/s.
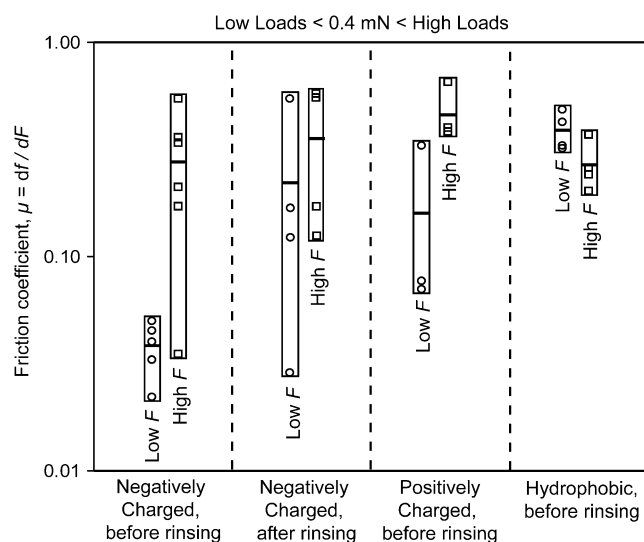
FIGURE 9   Friction coefficients μ measured for each type of surface (see "Statistical summary of friction measurements". Each point represents an independent experiment. For each group, a thick horizontal mark indicates the mean value $\langle\mu\rangle$, and a box shows the dispersion (scatter) of the experimental data. See also Table 1.

3. For negatively charged surfaces before rinsing, the mean friction coefficient measured for low loads, $\langle\mu\rangle = 0.038 \pm 0.018$, is about one order of magnitude lower than at high loads, $\langle\mu\rangle = 0.28 \pm 0.18$ ($p = 0.011$).
4. For hydrophobic surfaces before rinsing, the mean friction coefficient measured for low loads, $\langle\mu\rangle = 0.388 \pm 0.073$, is slightly higher than at high loads, $\langle\mu\rangle = 0.267 \pm 0.076$ ($p = 0.031$).

The mean value $\langle\mu\rangle = 0.16 \pm 0.15$ measured before rinsing for positively charged surfaces at low loads (Table 1) was heavily influenced by the result of one experiment that gave a value of $\mu > 0.3$—much higher than the values of $\mu \approx 0.075$ given by the other experiments. We therefore express the friction coefficient for positively charged surfaces at low loads as $\mu = 0.08$–0.3, to highlight the recurrence of a low-friction regime at low loads similar to the behavior observed with negatively charged surfaces.

DISCUSSION

Normal forces

The normal force measurements (Figs. 2, 3 a, 5, 7, and 8 a) show that LUB is a versatile antiadhesive: it adsorbs irreversibly to all the substrates considered and forms a layer protecting the substrates from further adsorption and from adhesion with other surfaces.

At the macroscopic scale, LUB is known to reduce cell adhesion and overgrowth on the cartilage surface, preventing malformation of the joint geometry and precocious deterioration of its articulation ability (11). LUB also prevents cartilage-cartilage adhesion, which would impair lubrication

and increase cartilage wear (10). Our work shows that the microscopic origin of these properties is the steric-entropic repulsion between the adsorbed layers when they overlap (Fig. 3 a). The repulsion is primarily entropic: it reflects the tendency of flexible protein molecules to coil randomly and resist the confinement that reduces the number of possible conformations (33,36). LUB acts like a polymeric anti-flocculant and antiadhesive of the type used in additives to colloidal suspensions to prevent aggregation (36), but with a large nonspecificity with respect to the type of surface.

The surface density of LUB on mica is expected to depend on the adsorption time and concentration. The adsorption appears to reach equilibrium within 3 h. For this adsorption time and for all the surfaces and concentrations (1/4 to above the physiological value) used in our experiments, the surface coverage of LUB adsorbed on mica was at the saturation value (see previous analysis of Figs. 2 and 3). The adsorbed layer is dense, with a surface mass density of 2.5–5 mg/m^2, which is comparable to the amount of LUB present at the surface of bovine cartilage surfaces (42), and to values reported for other, higher molecular weight and differently glycosylated mucins adsorbed on various surfaces after similar times (43–48).

The average distance between LUB molecules of $d \approx 10$ nm may be compared with the height of the adsorbed layer, $L = 60$–115 nm (Figs. 2, 3, 5, 7, and 8 a) and the extended length of the protein $l \approx 200$ nm, determined both from electron microscopy (13) and our bridging experiments (Fig. 3 b). We deduce that LUB molecules are not adsorbed as compact globules or flat "pancakes", but as brush-like layers of loops and tails elongated away from the surfaces (Fig. 9). This is why the forces are well described by the Alexander-de Gennes model (Figs. 3 a and 5 b), originally derived for a brush of uncharged end-grafted polymer chains. Long-range electrostatic interactions play a secondary role, being screened by the high salt concentration of the buffer solution. Moreover, a brush of loops is expected to be essentially equivalent to a brush of tails of the same height and with the same surface mass density (49). The average distance of $d \approx 10$ nm between proteins in the brush, obtained from refractive index measurements, is comparable to the average distance between grafting sites $s \approx 14$ nm obtained by fitting the Alexander-de Gennes equation to the measured forces. This suggests that LUB adsorbs to mica with only a few segments, each molecule exposing a few long loops and tails into the solution (Fig. 10).

Similar behavior has been observed for gelatin adsorbed on mica in high ionic strength (0.1 M) NaCl solutions (34). At the pH considered, any portion of the gelatin molecule can adsorb on mica. This leads to the formation of a "brush" layer of height 50 nm, which is about twice the radius of gyration of $R_g > 23$ nm. The adsorption energy is so high that the molecules have to adsorb close to each other ($d \approx 5$ nm) in the form of elongated tails and loops forming a crowded layer. As for LUB, the normal forces between
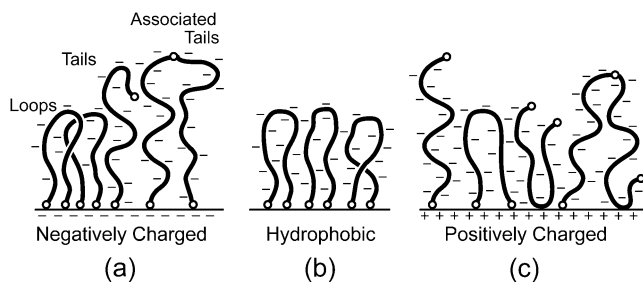
FIGURE 10 Proposed physisorbed configurations of LUB on (*a*) mica (negatively charged surface), (*b*) alkanethiol (hydrophobic surface), and (*c*) aminothiol (positively charged surface). Note the inter-LUB bonding in panels *a* and *c*.

gelatin-coated surfaces follow the theoretical profile given by Eq. 1, with a grafting distance *s* comparable to *d*.

SFA normal force measurements were previously reported on other (submaxillary and gastric) mucins with considerably higher molecular weights (4×10^6 and 10^7 g/mol), adsorbed on negatively charged hydrophilic (46,50) and hydrophobic (43) surfaces. For concentrations of mucin and electrolyte comparable to our work, some of these studies (43,50) show monotonically repulsive, nonhysteretic, and roughly exponentially-decaying forces. Based on experiments at different electrolyte concentrations it was concluded that the long-range force in these systems is of steric, not electrostatic, origin (43,46). It is instructive to subject the results obtained on rat gastric mucin (RGM) (43) to the same type of analysis performed above for LUB. The RGM had a larger molecular weight, $M_w = 10^7$ g/mol, than LUB, and a radius of gyration of $R_g = 190$ nm. The adsorption on the hydrophobic substrate was attributed to the interaction of several nonglycosylated sections (separating the glycosylated parts along the long protein chain), and was rapid and irreversible, leading to an average distance between molecules of $d = 75$ nm (adsorption density 3 mg/m^2). The normal force was purely repulsive and reproducible on a compression/decompression cycle. The range of the repulsion was ~150 nm and the force was roughly exponential at large separations, with a decay length of ~30 nm. At shorter separations, the repulsion rose considerably above the exponential profile measured at large separations. The repulsion did not depend on the ionic strength of the buffer solution, indicating a purely steric repulsion. However, within the measured range, the force in Malmsten et al. (43) does not seem to follow an Alexander-de Gennes profile. In conclusion, the structure of RGM on hydrophobized mica was different from LUB on mica and on the other substrates considered: more spaced out and less extended and, therefore, more "mushroom-like" than "brush-like".

In the case of LUB on negatively charged mica surfaces, the particular charge distribution on the LUB molecule (Fig. 1) appears to promote the adsorption of the positively charged globular ends of the molecule, and the formation of

single loops or tails, rather than a random adsorption of all parts of the molecule. The bridging experiments (Fig. 3 *b*) on mica suggest that the central part of the protein, the glycosylated and negatively charged "mucin" domain, may have a lower affinity for the mica surface than the end domains, which are globular and contain more positive than negative charges, as well as polar and hydrophobic groups (Fig. 1).

The shape of the shallow attractive well between a LUB-coated and a bare (uncoated) mica surface (Fig. 3 *b*) is typical of "telechelic" or "end-functionalized" polymers adsorbing only by their ends, such as PEG grafted on lipid bilayers in water by specific ligand-receptor interactions (40), or PEO-PS-PEO triblock polymers physisorbed on mica in toluene via their less soluble terminal PEO groups (51). In comparison, the attractive bridging force due to an adsorbing polymer of extended length *l* that can bind to a substrate at any portion of the chain decreases linearly with the separation or leads to a jump-out from a minimum at $D < l$, depending on the stiffness of the force-measuring spring (52).

Based on the above considerations, we propose the following model for the adsorption of LUB on mica and other surfaces (Figs. 2, 3, 5, 7, and 8 *a*) that helps understanding most, but not all, of the experimental results. LUB adsorbs on negatively charged mica in the form of end-grafted loops or single tails, with the central negatively charged and nonadsorbing domain pointing away from the surface (Fig. 10 *a*). Loops have an average height of $L \approx 60$ nm, approximately equal to 30% the extended molecular length, with an average distance $s \approx 14$ nm between adsorbed molecules. The repulsive force profile with the shortest range measured between two LUB-coated mica, $2L \approx 130$ nm (Figs. 2 and 3 *a*), is due to the steric interaction between brushes with a majority of loops. Force-distance curves with a larger range may be due to brushes of tails, which have not yet bent into loops (51). Tails disappear after rinsing the solution with pure buffer (Fig. 2 *c*), probably because they are more weakly bound than loops (one bound end instead of two). They also tend to disappear after repeated force runs at the same location and with longer incubation time, probably because both factors help the tails reach the more energetically favorable configuration of loops. However, the full interplay between loops and tails is not clear. For example, it is known that mucins tend to associate by their free ends (18), a behavior also observed for some synthetic telechelic polymers (53). Association of tails may produce larger loops (Fig. 10 *a*), that may contribute to create the repulsive force with the longer repulsive range. More experiments are necessary to understand why and when long- or short-range repulsion, or a "mixed" force profile, is observed.

When a LUB-coated mica surface approaches a bare (uncoated) mica surface (Fig. 3 *b*), first the free positively charged tail ends start adsorbing to the negative mica surface, creating a weak and poorly reproducible attraction at large separation distances $D = 50–150$ nm. Below 50–60 nm, the

normal steric-entropic repulsion takes over; but strong bridging bonds are also created by the tails and the opening up of some of the loops (since initially these reside only on one surface) (51). On separating the surfaces, the force is now much more attractive because of the much larger number of bridges than on approach. On separating to ∼100 nm, the repulsive force rapidly decreases due to the combined effects of the increasing bridging attraction and the decreasing steric repulsion. From 100 to 200 nm the bridges become stretched and their ends start detaching from the surfaces, giving rise to a broad but shallow energy minimum as previously explained in Wong et al. (40). The maximum bridging-adhesion distance of ∼200 nm (Fig. 3 b) is the maximum length of a stretched bridge before breaking, which agrees with the extended protein length (13). After all bridges have broken, the loops rapidly reform on the original LUB-coated mica surface, since successive compression/decompression cycles give similar forces as for the first cycle. This also means that protein transfer to the bare mica is limited, at least for the small number of compression/decompression cycles performed in our experiment (up to four per contact position).

The adsorption and normal forces measured for all the other substrates considered (positively charged poly-lysine and aminothiol, and hydrophobic alkanethiol surfaces) show features very similar to those observed for mica (Figs. 5, 7, and 8 a). The adsorption reaches saturation within 3 h and remains stable during rinsing. The forces between similar surfaces (i.e., both surfaces carrying LUB) are always repulsive and reversible, without any sign of hysteresis and with a range and decay comparable to the values measured for mica. We conclude that adsorption on substrates other than mica also leads to the formation of brushes of extended loops and tails with a comparable surface density. For hydrophobic alkanethiol surfaces, the force is always comparable to the repulsion with the shortest range of $2L ≈ 130$ nm measured for mica (Fig. 8 a). According to our model, this indicates that brushes on hydrophobic surfaces contain mainly single loops, rather than a mixture of loops and tails (Fig. 10 b). In fact, most of the hydrophobic groups in the LUB molecule are located in the end domains (14), that therefore are expected to have a stronger interaction with hydrophobic surfaces than the central mucin domain. As discussed further below, this hydrophobic interaction is much stronger than the other nonspecific protein-substrate interactions (39) and this favors the formation of a greater number of loops than on the other surfaces (51).

The adsorbed molecular configuration on positively charged poly-lysine and aminothiol surfaces was more difficult to determine. On one hand, fitting the Alexander-de Gennes equation to the repulsive force-distance data between poly-lysine layers gives a brush height of $L ≈ 65$ nm, suggestive of loops. On the other hand, adsorption on aminothiol-covered surfaces, which have a higher charge density than the poly-lysine layers, results in a scattered range of repul-

sion, probably because in this case the negatively charged central domain can also adsorb to the surface (Fig. 10 c), producing loops, tails, and ''trains'' with a broad height distribution.

Friction forces and wear

The friction and wear between the different LUB-coated surfaces studies were more varied than the normal forces, i.e., more specific to the type of surface considered. A summary of the friction coefficients, μ, measured for all experiments is given in Fig. 9. Table 1 gives the mean values, $\langle\mu\rangle$, and the standard deviations, σ, for each group of experiments.

For LUB layers confined between hydrophilic negatively charged mica surfaces the friction coefficient was low, $\langle\mu\rangle = 0.038 ± 0.018$, for low loads (Fig. 4 b). For LUB adsorbed on hydrophilic positively charged surfaces, i.e., mica coated with aminothiol or poly-lysine, a fairly low friction coefficient, $\mu ≈ 0.08$, is also observed at low loads (Fig. 6 b), although with a high dispersion in the data ($\mu = 0.08–0.3$). For both types of surfaces, the friction coefficient increases to $\mu = 0.2–0.6$ at higher pressures (Figs. 4 a and 6 a), leading to a breakdown of the boundary lubricant film, apparently via aggregation or pileup of the lubricin molecules. But surprisingly this ''breakdown'' or rearrangement of the protein layer did not result in damage (wear) of the underlying surfaces.

In contrast, the friction coefficient for hydrophobic alkanethiol surfaces is high already at low loads, $\langle\mu\rangle = 0.388 ± 0.073$, and slightly decreases at high loads to $\langle\mu\rangle = 0.267 ± 0.076$ (Fig. 8 b). Moreover, the load required to generate any visible damage to the LUB layers or the substrate is at least five times higher than for hydrophilic charged surface. Hence, it is clear that the strength of the adsorption and the details of the protein conformation in the boundary layers affect the friction forces, and wear damage, much more than they do the normal forces. Recent and old work on a variety of tribological systems show this to be a general effect (54).

The wear resistance of LUB layers adsorbed on different substrates mainly depends on the strength of the adsorption. It has been reported that LUB is more easily released from (negatively charged) glass surfaces during purification than from (hydrophobic) plastic containers (12). Our experiments with negatively charged mica show that at a load of $F > 0.5$ mN ($P > 6$ atm) the adsorption is not strong enough to resist shear that disrupt the molecule arrangement dictated by the surface. At the pH of our experiments, LUB contains roughly equal amounts of positive and negative charges, the isoelectric point being IEP = 7.8–8.1 (17). LUB adsorption on mica is due to van der Waals forces and to the electrostatic attraction between its positively charged residues and the negative charges on the mica surfaces. The charge density of mica is low, typically less that one electronic charge per

5 nm^2 (24). The attractive Coulombic forces are counteracted by the electrostatic repulsion between mica and the negatively charged residues. Additionally, there is competition for binding sites on the mica from the high concentration of anions and cations in the buffer solution, as well as from protons, even at neutral pH (24). The adsorption of LUB on negatively charged surfaces is thus expected to be weak. For positively charged surfaces (poly-lysine and aminothiol), the adsorption mechanism near the IEP is similar, which is reflected in the similarities in the normal forces, friction, and wear with the negatively charged mica surfaces.

In contrast, adsorption on a hydrophobic alkanethiol surface follows a very different mechanism that appears to be similar to the adsorption of amphiphilic molecules such as lipids, surfactants, certain proteins (41), and mucins (45), where the molecule binds to the hydrophobic surface via (some of) its hydrophobic residues, leaving the hydrophilic groups (charged, polar, and H-bonding) exposed to water. The effect is visible at the macroscopic scale, where initially hydrophobic (nonwater-wetted) surfaces become hydrophilic (water-wetted) and remain so for days after being in contact with LUB for a few hours (9). The hydrophobic-mediated binding of LUB to the hydrophobic surface is expected to be stronger than the electrostatic or ionic interactions (39), and there is no competition with the buffer ions for adsorbing sites. Thus, LUB brushes on hydrophobic surface can count on a stronger adsorption than on charged hydrophilic substrates to resist being sheared away. This explains the higher resistance to wear of the LUB layers adsorbed on alkanethiol surfaces.

Because LUB is a biological polyelectrolyte adsorbing in the form of a brush, it is natural to compare our results to what is observed for synthetic polyelectrolytes and block copolymers (19). Polyelectrolytes with functionalized end groups can be end-adsorbed on mica at high surface densities, in the form of stretched molecules (brushes). The normal forces between brushes are purely repulsive and exhibit surprisingly low friction coefficients, $\mu < 0.001$, at pressures up to several atmospheres (19). Such low friction requires low brush-brush interpenetration or entanglements, i.e., the formation of a sharp brush-brush interface under compression at physiological shear rates. In this regime, good brush-brush lubrication is provided by the hydration layers surrounding the charged polymer chains (19,20). At some critical pressure, the interpenetration suddenly increases and the friction increases, leading to wear of the brushes. Our results for LUB physisorbed on negatively and positively charged surfaces are reminiscent of this behavior, although with a much higher value of the friction coefficient $\mu > 0.02$. We believe that the lubricating properties of LUB are related to the presence of the heavily charged and hydrated mucin domain, which is present in the form of loops or tails at the brush-brush interface and it is bound to the surface by the end domains (Fig. 10). Indeed it has been observed that the friction increases after denaturing the hydrated sugars in the mucins domains (7,16) or after cutting away the end domains by enzymatic digestion (14).

It is difficult to explain how the adsorption strength and the protein conformation on different substrates influence the friction forces. Following the model proposed in Fig. 10, hydrophilic surfaces should bear a larger population of tails (Fig. 10, a and c) than hydrophobic surfaces (Fig. 10 b). At the same time, hydrophilic surfaces show a lower friction at low load (Figs. 4 b and 6 b) than hydrophobic surfaces (Fig. 8 b). Lubrication is generally improved by the presence of polymer brushes exposing tails (19,35,55). Here, however, we have both tails and loops. One may speculate that depending on the shear rate, tails can be forced to align along the shearing direction more easily than loops, creating a sharper interface between two brushes with little interpenetration and, therefore, low friction. A similar mechanism was previously proposed to explain the differences in friction measured for a cationic polyelectrolyte adsorbed on mica in different configurations: chains adsorbed in the form of open or stretched coils, projecting long extended tails into the solution, showed a lower friction coefficient than more compact coil (loops) configurations (56). In our case, the higher friction observed for hydrophobic surfaces at low loads could be due to the absence of tails on such surfaces (Fig. 10 b) or to a higher resistance of the loops to open into tails compared to hydrophilic surfaces.

Another interesting conclusion is that the friction coefficient is not a good indicator of whether wear will occur—again an observation that has been made before (57). We find that a high friction force does not necessarily induce surface damage, and conversely, that a low friction force does not guarantee that no damage will occur. Instead, our results show that damage to a lubricin layer, leading to the reorganization and/or aggregation of the glycoproteins on the surface, is brought about when the load (not the friction force) exceeds a certain critical value. For example, the friction measured for LUB on mica at low loads can be high (Fig. 4 a) or low (Fig. 4 b), but in all experiments the wear becomes measurable only above a load $F > 0.4$ mN. This force is related indirectly to the friction force via Amontons' Law: $F = f/\mu$. Thus, damage will occur at a low friction force if the friction coefficient μ is low, and at a high friction force if μ is high.

In the field of tribology, one of the basic equations describing the wear of rubbing surfaces is the Archard Equation (58):

$$W = kF/H, \qquad (3)$$

where W is the wear volume of material ''removed'' per unit length of sliding, k is a constant that depends on the surface or junction shape and the ''type'' of wear mechanism (plowing, cutting, abrading, micro-fracture, etc.), and H is the hardness. For elastic or plastic materials H is defined by $H = F/A$, where A is the area of the circle indented on a flat surface by a sphere of radius R pressed down by a load F.

In the case of a surface composed of lubricin or other soft biomaterial, H would be given by the repulsive force profile, $F(D)/R$. We thereby conclude that our observations on the critical conditions for wear are consistent with those of many conventional tribological systems. The biological implications are that wear may be determined more by the way the surface molecules are affected by the normal forces or pressures, than by the shear forces, although shearing appears to be a necessary condition for the damage to occur.

When extrapolated to the situation encountered in mammalian joints, our results indicate that LUB should be a good lubricant and wear protector of hydrophilic, preferably negatively charged, surfaces such as the surface of the outermost layer (''lamina splendens'') of the articular cartilage. This surface is believed to have a thin amorphous layer of hyaluronic acid, proteoglycans, and lipids that covers the underlying collagen of the cartilage (22). In light of our results, LUB should not lubricate an uncoated collagen surface, since this is at least partially hydrophobic (29). This may be biologically significant because the inner part of the cartilage that becomes exposed to the synovial fluid after joint damage is mainly composed of collagen (22). On the other hand, LUB should be a much better wear-protector for this hydrophobic surface than for hydrophilic surfaces.

It is important to stress that our LUB molecules were always physisorbed to the surfaces, rather than chemisorbed. LUB effectively lubricates our model surfaces only for loads $F < 0.5$ mN, corresponding to pressure below 6 atm, comparable to the pressure produced in real joints by light physical activities, such as walking, but not by strenuous activities, such as pressing or jumping that can produce transient pressures as high as 200 atm (1). Physisorbed molecules are much easier to dislodge and squeeze out when subjected to high shearing forces, unless these are laterally cross-linked, as recently shown for hyaluronic acid on lipid bilayers (57). LUB in vivo may well be strongly attached to the cartilage via complementary bonds. Indeed, LUB contains somatomedin B-like and homeopexin-like domains that are known to promote integrin-mediated attachment of cells to the extracellular matrix (10,11). It has been shown that LUB lacking these end domains does not lubricate effectively (12), probably because it does not bind strongly enough to the surface (7). The noncovalent binding of lubricin to our surfaces may be the reason for its unsatisfactory performance at high loads, and suggests that its binding to the cartilage surface may be mediated by much stronger bonds.

Another possibility is that LUB may interact with some other component in the synovial fluid, rather than on the surface, such as lipids (59) or hyaluronic acid (HA). HA is a high molecular weight polysaccharide that gives the synovial fluid its high viscosity and improves elasto-hydrodynamic lubrication of joints (6,57), but it is not a good boundary lubricant for cartilage (57,60). However, HA interacts with LUB and improves LUB lubrication in latex-on-glass contacts (61). HA may mediate the adsorption of LUB on cartilage or help the robustness of the adsorbed LUB layers, via cross-linking tethers. In other words, LUB probably acts synergistically with other molecules to produce the low friction and high wear resistance of healthy joints. Experiments are being completed to assess these hypotheses.

CONCLUSIONS

Lubricin adsorbs on both hydrophilic (charged) and hydrophobic surfaces to form polymer brush-like layers with extended loops and tails. The brush structure suppresses any adhesion between the surfaces and creates instead a soft (long-range) repulsion. This is the likely origin of the reported ability of lubricin to protect the surfaces of cartilage and tendons in joints from damage and prevent the excessive accumulation of cells, proteins, and other agents (10,11). A polymer brush-like behavior is observed in the normal and friction forces, which supports the idea that chemically bound polyelectrolyte brushes may serve as realistic models for biolubrication (19), and provide novel biocompatible, low-friction, low-wear coatings for the surfaces of joint implants (62). The lubrication and wear-protection of physisorbed lubricin involves nonspecific, noncovalent bonds, but the overall behavior is specific to the chemical nature of the substrate surface. The limited performance of physisorbed LUB suggests that optimal behavior, leading to ultralow friction and high resistance to wear, requires other contributions. These likely include fluid load support provided by the biphasic nature of cartilage (4) as well as complementary cross-linking interactions between lubricin and some other component in the synovial fluid and/or on the cartilage surface.

REFERENCES

1. Morrell, K. C., W. A. Hodge, D. E. Krebs, and R. W. Mann. 2005. Corroboration of in vivo cartilage pressures with implications for synovial joint tribology and osteoarthritis causation. *Proc. Natl. Acad. Sci. USA.* 102:14819–14824.

2. Forster, H., and J. Fisher. 1996. The influence of loading time and lubricant on the friction of articular cartilage. *Proc. Inst. Mech. Eng.* 210:109–119.

3. Kuettner, K. E., R. Schleyerbach, J. G. Peyron, and V. C. Hascall, editors. 1991. Articular Cartilage and Osteoarthritis. Raven, New York.

4. McCutchen, C. W. 1962. The frictional properties of animal joints. *Wear.* 5:1–17.

5. Mow, V. C., and W. M. Lai. 1980. Recent developments in synovial joint biomechanics. *SIAM Review.* 22:275–317.

6. Radin, E. L., D. A. Swann, and P. A. Weisser. 1970. Separation of a hyaluronate-free lubricating fraction from synovial fluid. *Nature.* 228: 377–378.

7. Swann, D. A., R. B. Hendren, E. L. Radin, S. L. Sotman, and E. A. Duda. 1981. The lubricating activity of synovial fluid glycoproteins. *Arthritis Rheum.* 24:22–30.

8. Swann, D. A., S. Sotman, M. Dixon, and C. Brooks. 1977. The isolation and partial characterization of the major glycoprotein (LGP-I) from the articular lubricating fraction from bovine synovial fluid. *Biochem. J.* 161:473–485.

9. Jay, G. D. 1992. Characterization of a bovine synovial fluid lubricating factor. I. Chemical, surface activity and lubricating properties. *Connect. Tissue Res.* 28:71–88.

10. Schaefer, D. B., D. Wendt, M. Moretti, M. Jakob, G. D. Jay, M. Heberer, and I. Martin. 2004. Lubricin reduces cartilage-cartilage integration. *Biorheology.* 41:503–508.

11. Rhee, D. K., J. Marcelino, M. Baker, Y. Gong, P. Smits, V. Lefebvre, G. D. Jay, M. Stewart, H. Wang, M. L. Warman, and J. D. Carpten. 2005. The secreted glycoprotein lubricin protects cartilage surfaces and inhibits synovial cell overgrowth. *J. Clin. Invest.* 115:622–631.

12. Jay, G. D. 2004. Lubricin and surfacing of articular joints. *Curr. Opin. Orthop.* 15:355–359.

13. Swann, D. A., H. S. Slayter, and F. H. Silver. 1981. The molecular structure of lubricating glycoprotein-I, the boundary lubricant for articular cartilage. *J. Biol. Chem.* 256:5921–5925.

14. Jay, G. D., U. Tantravahi, D. E. Britt, H. J. Barrach, and C. J. Cha. 2001. Homology of lubricin and superficial zone protein (SZP): products of megakaryocyte stimulating factor (MSF) gene expression by human synovial fibroblasts and articular chondrocytes localized to chromosome 1q25. *J. Orthop. Res.* 19:677–687.

15. Jay, G. D., D. E. Britt, and C. J. Cha. 2000. Lubricin is a product of megakaryocyte stimulating factor gene expression by human synovial fibroblasts. *J. Rheumatol.* 27:594–600.

16. Jay, G. D., D. A. Harris, and C. J. Cha. 2001. Boundary lubrication by lubricin is mediated by O-linked $\beta(1–3)$Gal-GalNAc oligosaccharides. *Glycoconj. J.* 18:807–815.

17. Jay, G. D. 1990. Joint lubrication: a physico-chemical study of a purified lubricating factor from bovine synovial fluid. PhD thesis. State University of New York, Stony Brook, NY.

18. Bansil, R., E. Stanley, and J. T. LaMont. 1995. Mucin biophysics. *Annu. Rev. Physiol.* 57:635–657.

19. Raviv, U., S. Giasson, N. Kampf, J. F. Gohy, R. Jerome, and J. Klein. 2003. Lubrication by charged polymers. *Nature.* 425:163–165.

20. Raviv, U., and J. Klein. 2002. Fluidity of bound hydration layers. *Science.* 297:1540–1543.

21. Jay, G. D., K. Haberstroh, and C. J. Cha. 1998. Comparison of the boundary-lubricating ability of bovine synovial fluid, lubricin, and Healon. *J. Biomed. Mater. Res.* 40:414–418.

22. Teshima, R., M. Ono, Y. Yamashita, H. Hirakawa, K. Nawata, and Y. Morio. 2004. Immunohistochemical collagen analysis of the most superficial layer in adult articular cartilage. *J. Orthop. Sci.* 9:270–273.

23. Sokoloff, L, editor. 1980. The Joints and Synovial Fluid, Vol. 2. Academic Press, New York.

24. Pashley, R. M. 1981. DLVO and hydration forces between mica surfaces in Li$^+$, Na$^+$, K$^+$, and Cs$^+$ electrolyte solutions: a correlation of double-layer and hydration forces with surface cation exchange properties. *J. Colloid Interface Sci.* 83:531–546.

25. Pashley, R. M. 1985. Electromobility of mica particles dispersed in aqueous solutions. *Clays Clay Miner.* 33:193–199.

26. Alcantar, N. A., C. Park, J. M. Pan, and J. N. Israelachvili. 2003. Adhesion and coalescence of ductile metal surfaces and nanoparticles. *Acta Materialia.* 51:31–47.

27. Ruths, M., M. Heuberger, V. Scheumann, J. Hu, and W. Knoll. 2001. Confinement-induced film thickness transitions in liquid crystals between two alkanethiol monolayers on gold. *Langmuir.* 17:6213–6219.

28. Heuberger, M. 2001. The extended surface forces apparatus. Part I. Fast spectral correlation interferometry. *Rev. Sci. Instrum.* 72:1700–1707.

29. Chappuis, J., I. A. Sherman, and A. W. Neumann. 1983. Surface tension of animal cartilage as it relates to friction in joints. *Ann. Biomed. Eng.* 11:435–449.

30. Israelachvili, J. N., and P. M. McGuiggan. 1990. Adhesion and short-range forces between surfaces. Part I. New apparatus for surface force measurements. *J. Mater. Res.* 5:2223–2231.

31. Israelachvili, J. N. 1973. Thin film studies using multiple-beam interferometry. *J. Colloid Interface Sci.* 44:259–272.

32. Luengo, G., F.-J. Schmitt, R. Hill, and J. Israelachvili. 1997. Thin film rheology and tribology of confined polymer melts: contrast with bulk properties. *Macromolecules.* 30:2482–2494.

33. De Gennes, P. G. 1987. Polymers at an interface: a simplified view. *Adv. Colloid Interface Sci.* 27:189–209.

34. Kamiyama, Y., and J. Israelachvili. 1992. Effect of pH and salt on the adsorption and interactions of an amphoteric polyelectrolyte. *Macromolecules.* 25:5081–5088.

35. Klein, J., E. Kumacheva, D. Mahalu, D. Perahia, and L. J. Fetters. 1994. Reduction of frictional forces between solid surfaces bearing polymer brushes. *Nature.* 370:634–636.

36. Israelachvili, J. N. 1991. Intermolecular and Surface Forces. Academic Press, London, UK.

37. Klein, J. 1983. Forces between mica surfaces bearing adsorbed macromolecules in liquid media. *J. Chem. Soc. Faraday Transactions I.* 79:99–118.

38. Ball, V., and J. J. Ramsden. 1998. Buffer dependence of refractive index increments of protein solutions. *Biopolymers.* 46:489–492.

39. Leckband, D., and J. N. Israelachvili. 2001. Intermolecular forces in biology. *Q. Rev. Biophys.* 34:105–267.

40. Wong, J. Y., T. L. Kuhl, J. N. Israelachvili, N. Mullah, and S. Zalipsky. 1997. Direct measurement of a tethered ligand-receptor interaction potential. *Science.* 275:820–822.

41. Leckband, D., Y.-L. Chen, J. Israelachvili, H. H. Wickman, M. Fletcher, and R. Zimmerman. 1993. Measurements of conformational changes during adhesion of lipid and protein (polylysine and S-layer) surfaces. *Biotechnol. Bioeng.* 42:167–177.

42. Schumacher, B. L., T. A. Schmidt, M. S. Voegtline, A. C. Chen, and R. L. Sah. 2005. Proteoglycan 4 (PRG4) synthesis and immunolocalization in bovine meniscus. *J. Orthop. Res.* 23:562–568.

43. Malmsten, M., E. Blomberg, P. Claesson, I. Carlstedt, and I. Ljusegren. 1992. Mucin layers on hydrophobic surfaces studied with ellipsometry and surface force measurements. *J. Colloid Interface Sci.* 151:579–590.

44. Shi, L., R. Ardehali, K. D. Caldwell, and P. Valint. 2000. Mucin coating on polymeric material surfaces to suppress bacterial adhesion. *Colloids Surf. B Biointerfaces.* 17:229–239.

45. Shi, L., and K. D. Caldwell. 2000. Mucin adsorption to hydrophobic surfaces. *J. Colloid Interface Sci.* 224:372–381.

46. Perez, E., and J. E. Proust. 1987. Forces between mica surfaces covered with adsorbed mucin across aqueous solution. *J. Colloid Interface Sci.* 118:182–191.

47. Dedinaite, A., and L. Bastardo. 2002. Interactions between mucin and surfactants at solid-liquid interfaces. *Langmuir.* 18:9383–9392.

48. Lee, S., M. Müller, K. Rezwan, and N. D. Spencer. 2005. Porcine gastric mucin (PGM) at the water/poly(dimethylsiloxane) (PDMS) interface: influence of pH and ionic strength on its conformation, adsorption, and aqueous lubrication properties. *Langmuir.* 21:8344–8353.

49. Milner, S. T., and T. A. Witten. 1992. Bridging attraction by telechelic polymers. *Macromolecules.* 25:5495–5503.

50. Dedinaite, A., M. Lundin, L. Macakova, and T. Auletta. 2005. Mucin-chitosan complexes at the solid-liquid interface: multilayer formation and stability in surfactant solutions. *Langmuir.* 21:9502–9509.

51. Dai, L., and C. Toprakcioglu. 1992. End-adsorbed triblock copolymer chains at the liquid-solid interface: bridging effects in good solvent. *Macromolecules.* 25:6000–6006.

52. Ruths, M., J. N. Israelachvili, and H. J. Ploehn. 1997. Effects of time and compression on the interactions of adsorbed polystyrene layers in a near-theta solvent. *Macromolecules*. 30:3329–3339.

53. Eiser, E., J. Klein, T. A. Witten, and L. J. Fetters. 1999. Shear of telechelic brushes. *Phys. Rev. Lett.* 82:5076–5079.

54. Israelachvili, J., N. Maeda, K. J. Rosenberg, and M. Akbulut. 2005. Effects of sub-Ångstrom (pico-scale) structure of surfaces on adhesion, friction, and bulk mechanical properties. *J. Mater. Res.* 20:1952–1972.

55. Pelletier, E., G. F. Belder, G. Hadziioannou, and A. Subbotin. 1997. Nanorheology of adsorbed diblock copolymer layers. *Journal de Physique II*. 7:271–283.

56. Qian, L., M. Charlot, E. Perez, G. Luengo, A. Potter, and C. Cazeneuve. 2004. Dynamic friction by polymer/surfactant mixtures adsorbed on surfaces. *J. Phys. Chem. B.* 108:18608–18614.

57. Benz, M., N. H. Chen, and J. Israelachvili. 2004. Lubrication and wear properties of grafted polyelectrolytes, hyaluronan and hylan, measured in the surface forces apparatus. *J. Biomed. Mater. Res. A.* 71:6–15.

58. Tylczak, J. H. 1992. Abrasive wear. *In* Friction, Lubrication and Wear Technology. ASM Handbook. ASM International, Materials Park, OH. 184–190.

59. Ozturk, H. E., K. K. Stoffel, C. F. Jones, and G. W. Stachowiak. 2004. The effect of surface-active phospholipids on the lubrication of osteoarthritic sheep knee joints: friction. *Tribology Letters*. 16: 283–289.

60. Swann, D. A., E. L. Radin, M. Nazimiec, P. A. Weisser, N. Curran, and G. Lewinnek. 1974. Role of hyaluronic acid in joint lubrication. *Annals of the Rheumatoid Diseases*. 33:318–326.

61. Jay, G. D., B. P. Lane, and L. Sokoloff. 1992. Characterization of a bovine synovial fluid lubricating factor. III. The interaction with hyaluronic acid. *Connect. Tissue Res.* 28:245–255.

62. Moro, T., Y. Takatori, K. Ishihara, T. Konno, Y. Takigawa, T. Matsushita, U. I. Chung, K. Nakamura, and H. Kawaguchi. 2004. Surface grafting of artificial joints with a biocompatible polymer for preventing periprosthetic osteolysis. *Nat. Mater.* 3:829–836.